

1       **Supplement to: Stationary waves weaken and delay the near-surface**  
2                   **response to stratospheric ozone depletion**

3                                   Chaim I. Garfinkel\*

4    *The Hebrew University of Jerusalem, Institute of Earth Sciences, Edmond J. Safra Campus, Givat*  
5                                   *Ram, Jerusalem, Israel*

6                                   Ian White

7    *The Hebrew University of Jerusalem, Institute of Earth Sciences, Edmond J. Safra Campus, Givat*  
8                                   *Ram, Jerusalem, Israel*

9                                   Edwin P. Gerber

10                                *Courant Institute of Mathematical Sciences, New York University, New York, USA*

11                                Seok-Woo Son

12                                *School of Earth and Environmental Sciences, Seoul National University, Seoul, South Korea*

13                                Martin Jucker

14                                *Climate Change Research Centre and ARC Centre of Excellence for Climate Extremes,*  
15                                    *University of New South Wales, Sydney, Australia*

16    \*Corresponding author address: Chaim I. Garfinkel, The Hebrew University of Jerusalem, Institute  
17    of Earth Sciences, Edmond J. Safra Campus, Givat Ram, Jerusalem, Israel.

<sup>18</sup> E-mail: [chaim.garfinkel@mail.huji.ac.il](mailto:chaim.garfinkel@mail.huji.ac.il)

## ABSTRACT

19 Figure S1 shows the climatological zonal mean zonal wind in STAT and  
20 AQUA80. Figure S2 shows the zonal wind at 850hPa response to ozone de-  
21 pletion in STAT and AQUA80. Figure S3 shows the Eliassen-Palm flux di-  
22 vergence response to ozone depletion in AQUA80 and STAT, while Figure  
23 S7 is similar but for a stratospheric diabatic cooling perturbation. Figure S4  
24 shows the climatological Eliassen-Palm flux for reference. The main body  
25 documents some aspects of the response when an ozone hole is placed in the  
26 Northern Hemisphere, and Figure S5 shows more. Figure S6 shows the trans-  
27 formed Eulerian mean momentum budget for AQUA80. Figure S8 shows the  
28 response to ozone when the jet latitude is pushed poleward for the AQUA80  
29 configuration.

30 *Acknowledgments.* CIG, IW, and ME acknowledge the support of a European Research Coun-  
31 cil starting grant under the European Union Horizon 2020 research and innovation programme  
32 (grant agreement number 677756). EPG acknowledges support from the US NSF through grant  
33 AGS 1852727. MJ acknowledges support from the Australian Research Council (ARC) Centre  
34 of Excellence for Climate Extremes (CE170100023) and ARC grant FL 150100035. SWS was  
35 supported by the National Research Foundation of Korea (NRF) grant funded by the Korea gov-  
36 ernment (Ministry of Science and ICT 2017R1E1A1A01074889).

### 37 **References**

38 Garfinkel, C. I., I. White, E. P. Gerber, and M. Jucker, 2020: The impact of sst biases in the  
39 tropical east pacific and agulhas current region on atmospheric stationary waves in the southern  
40 hemisphere. *Journal of Climate*, **33** (21), 9351–9374.

41 **LIST OF FIGURES**

42 **Fig. S1.** Climatology of zonal wind in the postindustrial control run of STAT (bottom) and AQUA80  
 43 (top) for the three periods focused on in the other figures. The zero-line is magenta. . . . . 6

44 **Fig. S2.** Zonal wind response [hole - PI] at 850hPa in STAT and AQUA80. . . . . 7

45 **Fig. S3.**  $EP_z$  for wavenumber-1,  $EP_y$  for all wavenumbers, and EPFD for all wavenumbers for the  
 46 [ozone hole-PI] runs in (left) days 1-30 after branching, i.e. October; (middle) days 31 to  
 47 70; (right) days 71 to 120. Top three rows are for STAT, and the bottom three rows are for  
 48 AQUA80. For the EPFD, we show the  $EP_z$  and  $EP_y$  components for all wavenumber with  
 49 arrows with the  $EP_z$  enhanced by a factor of 50; above 93hPa, the arrows are multiplied by  
 50 a factor of 5. . . . . 8

51 **Fig. S4.**  $EP_z$  for wavenumber-1,  $EP_y$  for all wavenumbers, and EPFD for all wavenumbers for the  
 52 PI climatology in STAT and AQUA80. Other conventions intentionally follow Figure S3,  
 53 which leads to saturation of colors in the troposphere. . . . . 9

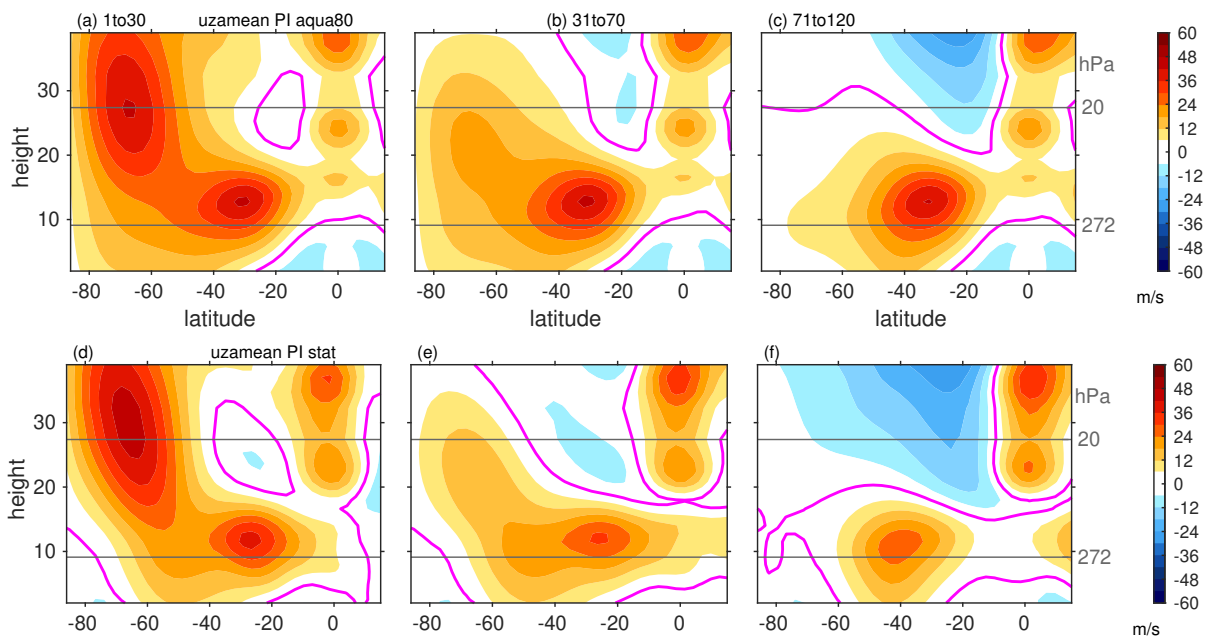
54 **Fig. S5.** Zonal-mean responses of temperature and zonal wind for a NH ozone hole branch ensemble  
 55 starting on March 1st. . . . . 10

56 **Fig. S6.** TEM momentum budget for the [ozone hole-PI] aquaplanet runs, with “Antarctic” albedo  
 57 equal to 0.8 in (left) days 1-30 after branching, i.e. October; (middle) days 31 to 70; (right)  
 58 days 71 to 120. (a-c) total wind tendency; (d-f) sum of all terms; (g-i) eddy forcing terms  
 59 ( $u'v'$  and  $u'w'$ ); (j-l) coriolis torque; (m-o) sum of eddy forcing and coriolis torque; (p-r)  
 60 gravity wave drag; (s-u) advection of mean zonal wind. Note that the color-bar for (g-i)  
 61 and (j-l) differ from that in (m-o) due to the strong cancellation between eddy forcing and  
 62 coriolis torque (as expected). . . . . 11

63 **Fig. S7.** As in Figure S3 but for the diabatic forcing experiments. . . . . 12

64 **Fig. S8.** As in Figure 6 of the main text but for a jet latitude  $7^\circ$  further poleward achieved by im-  
 65 posing a north-south gradient in midlatitude ocean heat transport following equation A8 of  
 66 Garfinkel et al. (2020). . . . . 13

67 **Fig. S9.** Surface temperature anomalies associated with a 1 std dev anomaly of the SAM in STAT  
 68 and in AQUA80. Note that surface temperature warming over South America are present  
 69 as expected for both, however STAT does not simulate the expected surface cooling over  
 70 Antarctica, consistent with the lack of an Antarctic cooling signal in response to ozone  
 71 depletion. The colorbars differ for the top and bottom row. . . . . 14



72 Fig. S1. Climatology of zonal wind in the postindustrial control run of STAT (bottom) and AQUA80 (top) for  
 73 the three periods focused on in the other figures. The zero-line is magenta.

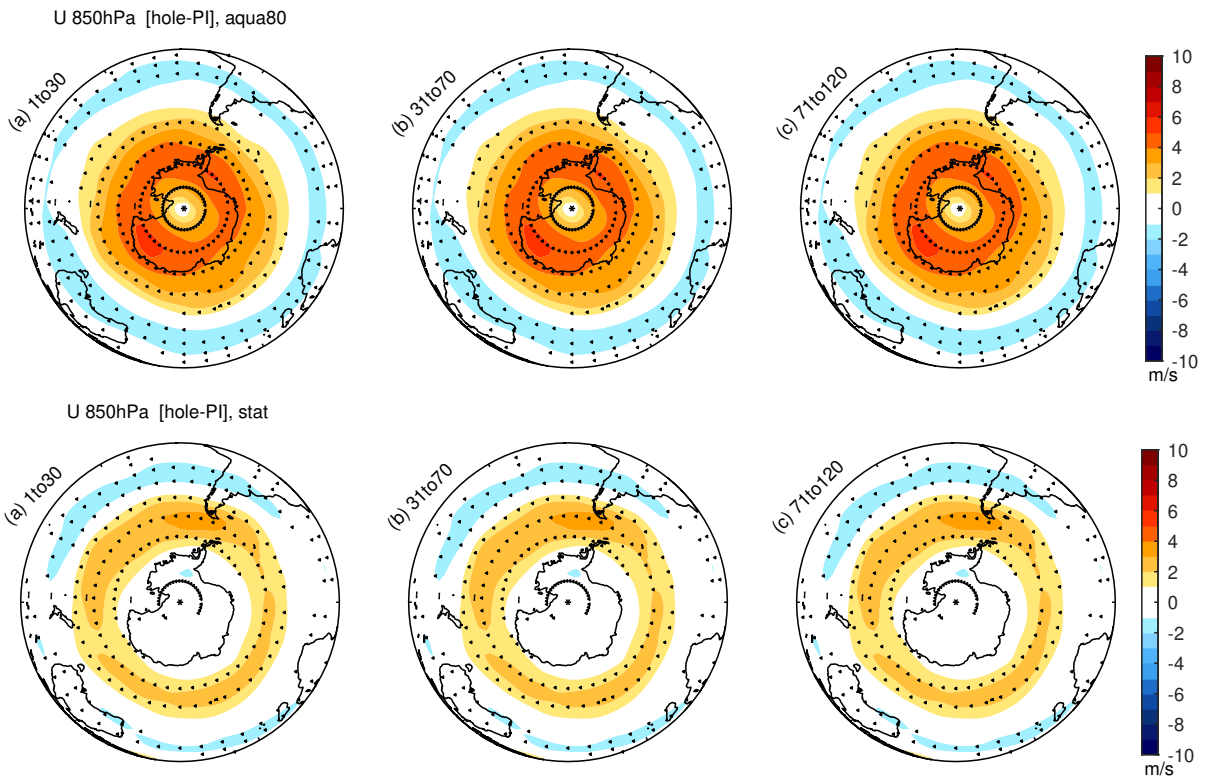
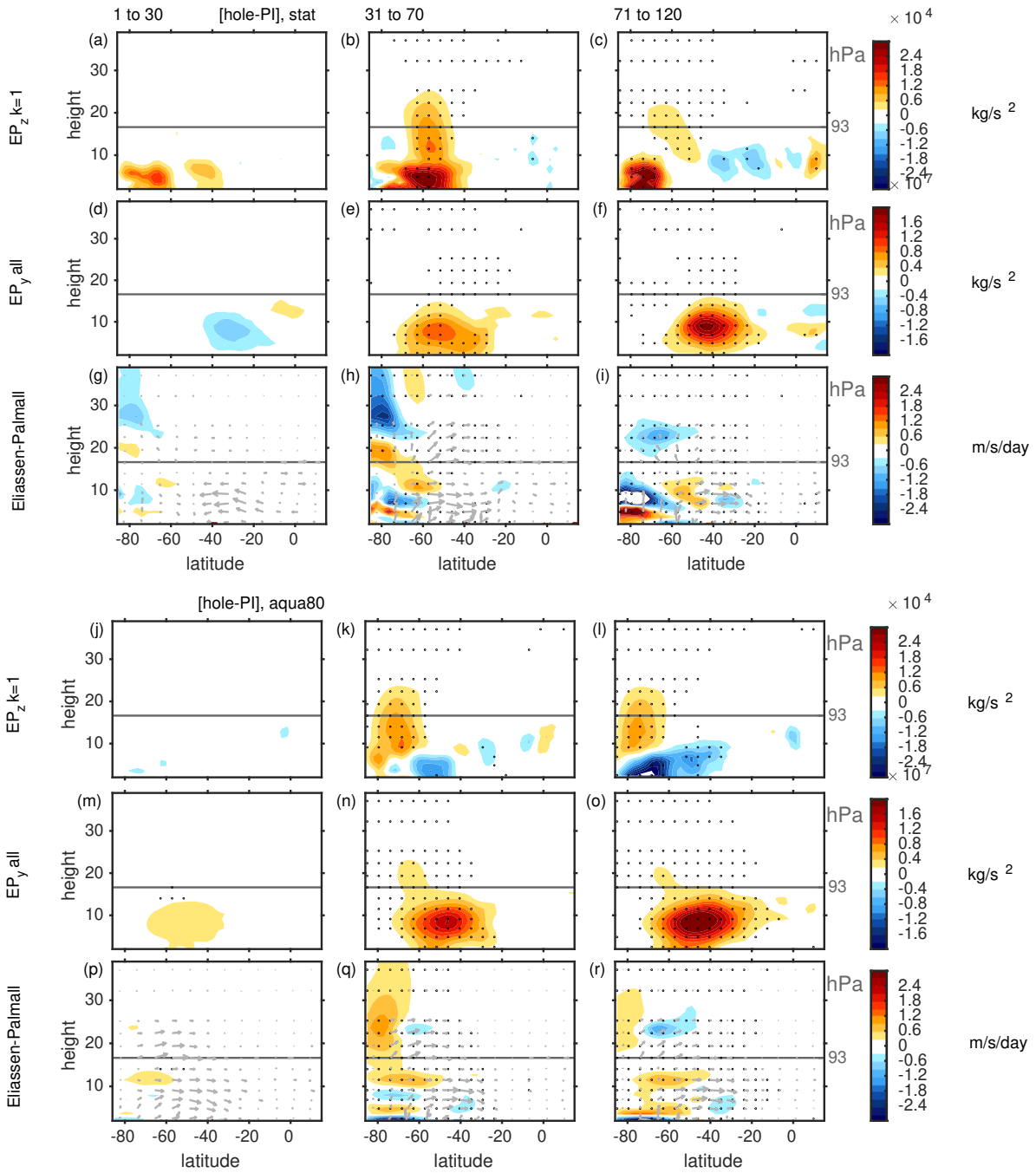
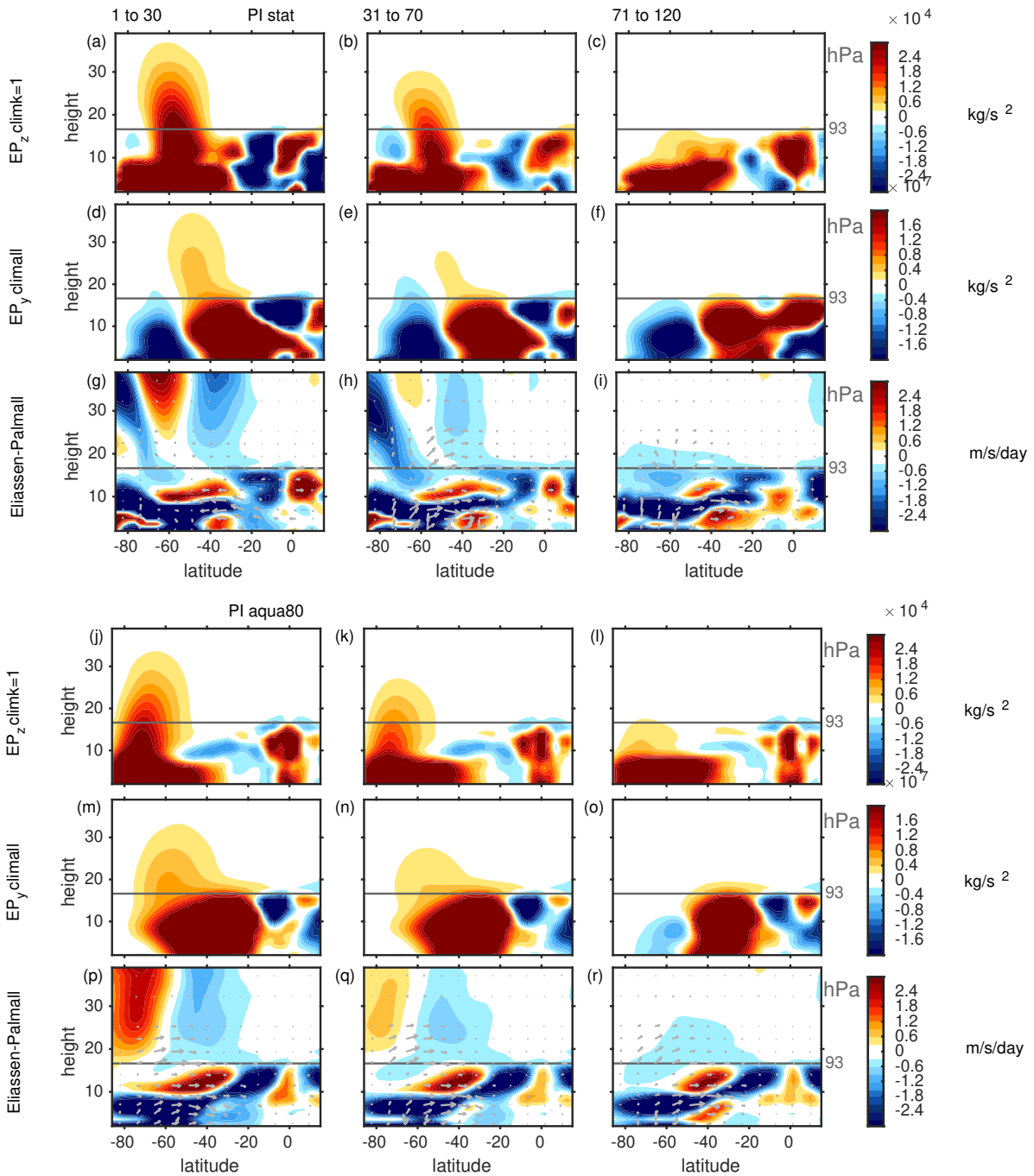


Fig. S2. Zonal wind response [hole - PI] at 850hPa in STAT and AQUA80.

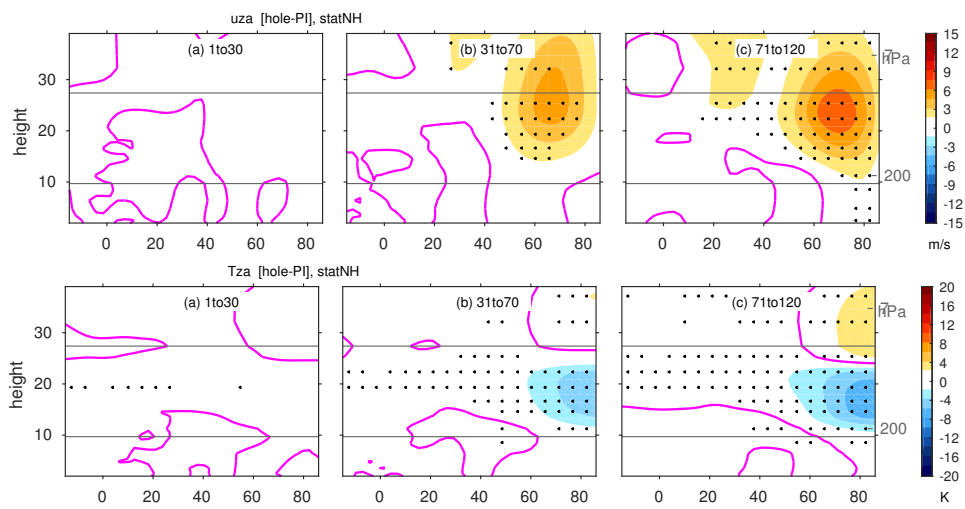


74 Fig. S3. EP<sub>z</sub> for wavenumber-1, EP<sub>y</sub> for all wavenumbers, and EPFD for all wavenumbers for the [ozone  
 75 hole-PI] runs in (left) days 1-30 after branching, i.e. October; (middle) days 31 to 70; (right) days 71 to 120.  
 76 Top three rows are for STAT, and the bottom three rows are for AQUA80. For the EPFD, we show the EP<sub>z</sub> and  
 77 EP<sub>y</sub> components for all wavenumber with arrows with the EP<sub>z</sub> enhanced by a factor of 50; above 93hPa, the  
 78 arrows are multiplied by a factor of 5.

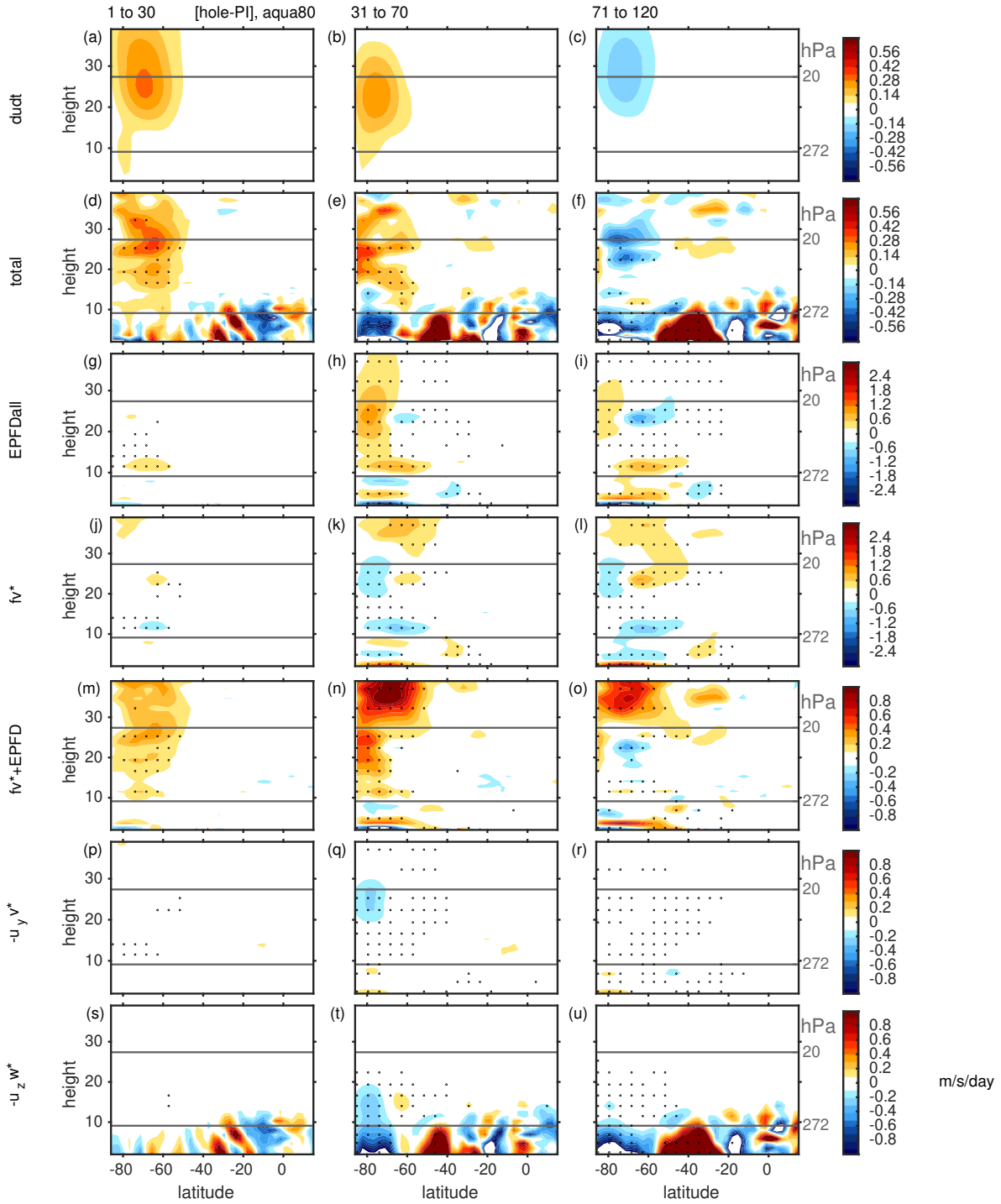




79 Fig. S4.  $EP_z$  for wavenumber-1,  $EP_y$  for all wavenumbers, and EPFD for all wavenumbers for the PI clima-  
 80 tology in STAT and AQUA80. Other conventions intentionally follow Figure S3, which leads to saturation of  
 81 colors in the troposphere.



82 Fig. S5. Zonal-mean responses of temperature and zonal wind for a NH ozone hole branch ensemble starting  
 83 on March 1st.



84 Fig. S6. TEM momentum budget for the [ozone hole-PI] aquaplanet runs, with “Antarctic” albedo equal to  
 85 0.8 in (left) days 1-30 after branching, i.e. October; (middle) days 31 to 70; (right) days 71 to 120. (a-c) total  
 86 wind tendency; (d-f) sum of all terms; (g-i) eddy forcing terms ( $u'v'$  and  $u'w'$ ); (j-l) coriolis torque; (m-o) sum  
 87 of eddy forcing and coriolis torque; (p-r) gravity wave drag; (s-u) advection of mean zonal wind. Note that the  
 88 color-bar for (g-i) and (j-l) differ from that in (m-o) due to the strong cancellation between eddy forcing and  
 89 coriolis torque (as expected).

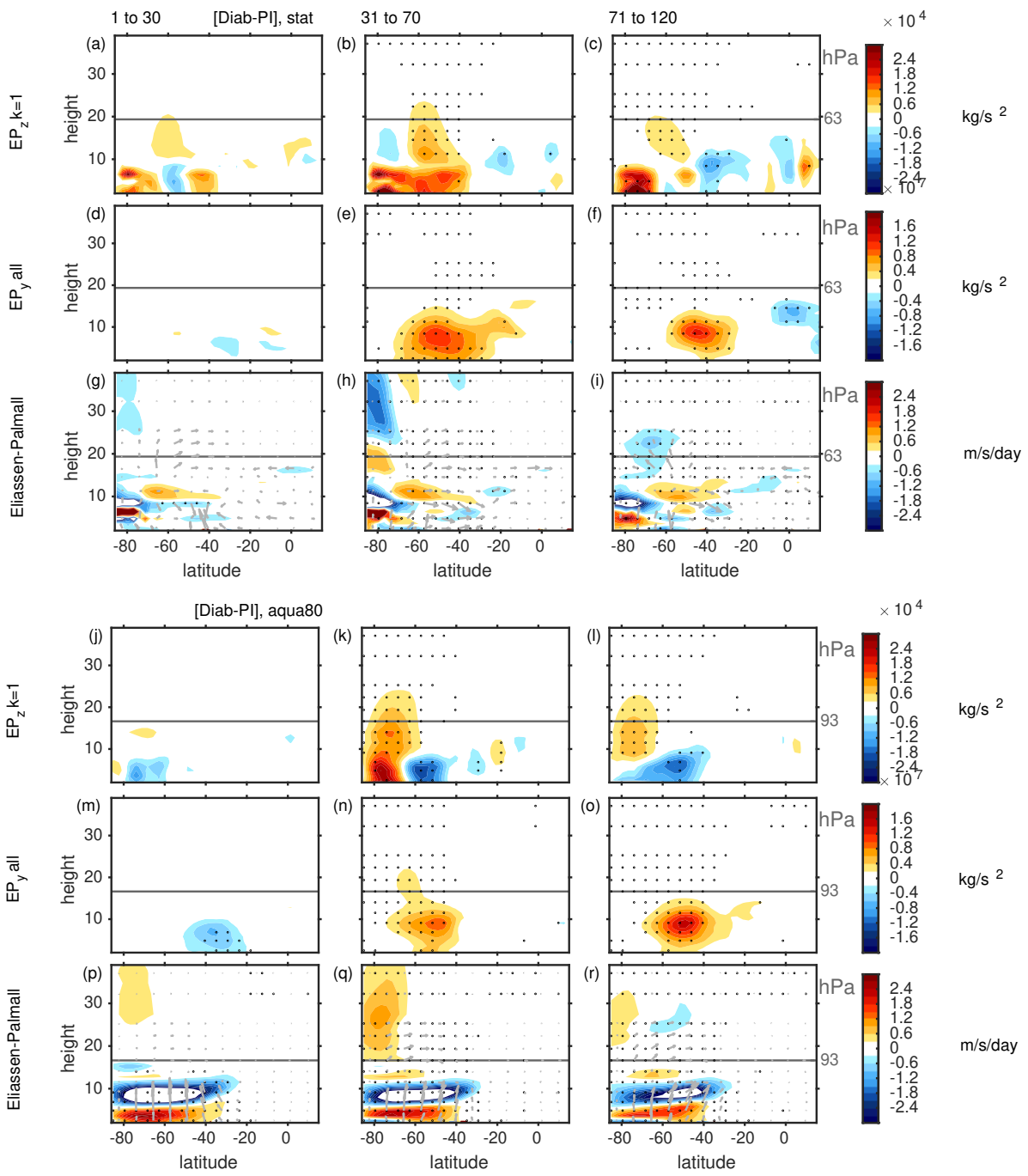
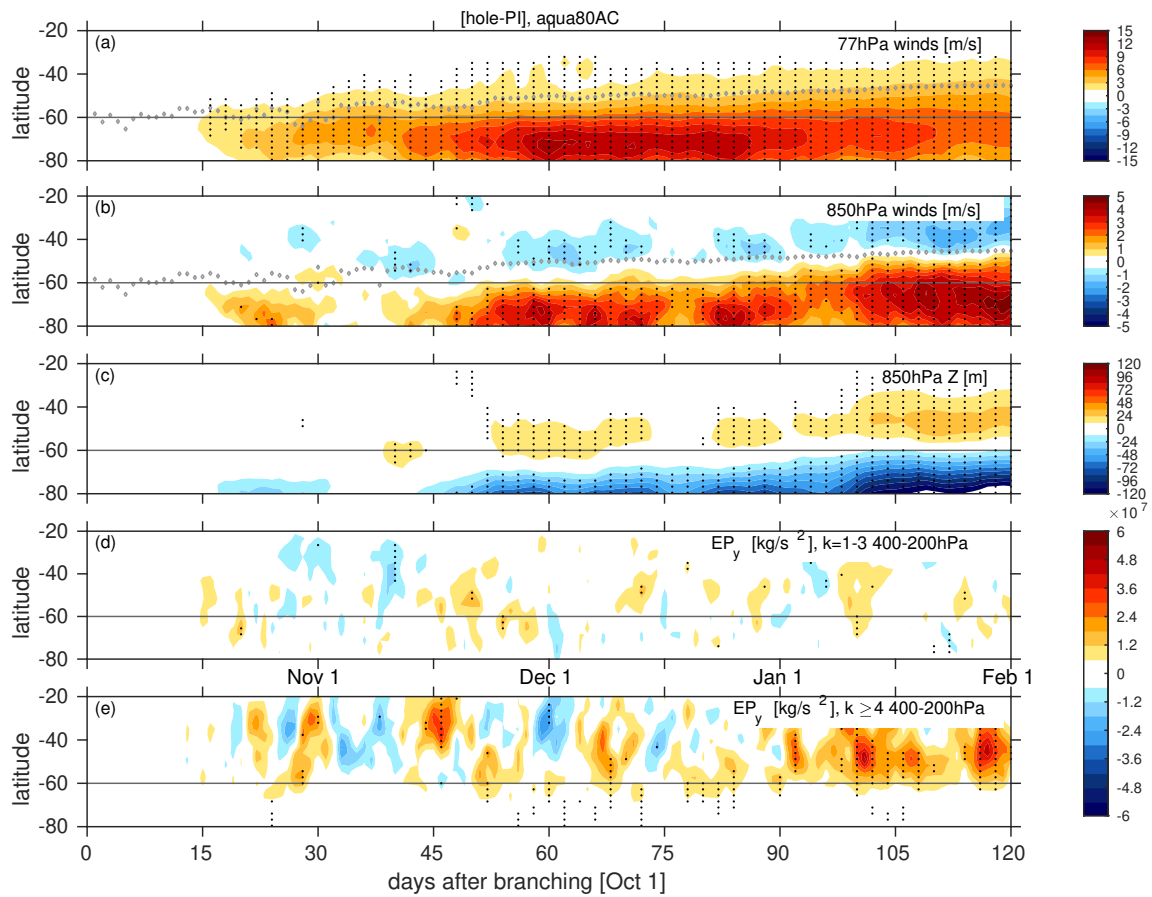
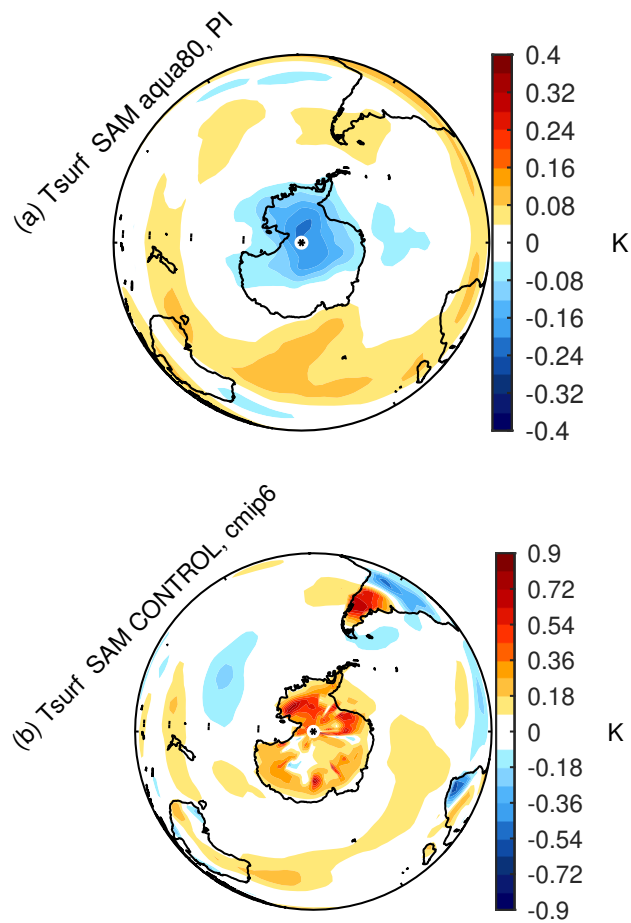


Fig. S7. As in Figure S3 but for the diabatic forcing experiments.



90 Fig. S8. As in Figure 6 of the main text but for a jet latitude  $7^\circ$  further poleward achieved by imposing a  
 91 north-south gradient in midlatitude ocean heat transport following equation A8 of Garfinkel et al. (2020).



92 Fig. S9. Surface temperature anomalies associated with a 1 std dev anomaly of the SAM in STAT and in  
 93 AQUA80. Note that surface temperature warming over South America are present as expected for both, however  
 94 STAT does not simulate the expected surface cooling over Antarctica, consistent with the lack of an Antarctic  
 95 cooling signal in response to ozone depletion. The colorbars differ for the top and bottom row.